Josephson effect due to the long-range odd-frequency triplet superconductivity in SFS junctions with Néel domain walls

Ya. V. Fominov,[1,*] A. F. Volkov,[2,3,†] and K. B. Efetov[2,1]

[1]*L. D. Landau Institute for Theoretical Physics RAS, 119334 Moscow, Russia*
[2]*Theoretische Physik III, Ruhr-Universität Bochum, D-44780 Bochum, Germany*
[3]*Institute of Radioengineering and Electronics of the Russian Academy of Sciences, 103907 Moscow, Russia*

We consider a SFS Josephson junction made of two superconductors S and a multidomain ferromagnet F with an in-plane magnetization. We assume that the neighboring domains of the ferromagnet are separated by Néel domain walls. An odd-frequency triplet long-range component of superconducting correlations arises in the domain walls and spreads into the domains over a long distance of the order $\xi_T = \sqrt{D/2\pi T}$, where D is the diffusion coefficient (dirty limit is implied). We calculate the contribution of this component to the Josephson current in the situation when conventional short-range components exponentially decay over the thickness of the F layer and can be neglected. In the limit when the thickness of the F layer is much smaller than the penetration length of the long-range component, we find that the junction is in the π state. We also analyze a correction to the density of states due to the long-range triplet component.

I. INTRODUCTION

The past decade was marked by a rapid growth of interest to the study of hybrid superconductor-ferromagnet (SF) structures (see, for example, Refs. 1–3). New physical phenomena arising in these systems originate from a nontrivial interplay of competing orders in superconductors and ferromagnets. On one side, electron-electron interactions lead in superconductors to formation of Cooper pairs consisting of two electrons with opposite spins. On the other side, the exchange interaction in ferromagnets tends to align the electron spins parallel to each other. In SF structures these two types of interactions are spatially separated and can coexist despite much greater value of the exchange energy h in comparison with the superconducting gap Δ.

Due to the proximity effect[4] the superconducting correlations penetrate into the ferromagnet in SF structures. The condensate wave function f penetrates into the ferromagnet with a uniform magnetization **M** over a distance of the order of the "exchange length" $\xi_h = \sqrt{D/h}$.[1,2] The condensate wave function decays in F in a nonmonotonic way as $f(x) \sim \exp(-x/\xi_h)\cos(x/\xi_h)$: it oscillates in space and decreases exponentially. This nonmonotonic behavior of $f(x)$ leads, in particular, to a π state in SFS Josephson junctions[1,2,5–10] characterized by a negative critical current I_c in the Josephson current-phase relation $I(\varphi) = I_c \sin\varphi$.

If the magnetization in the ferromagnet is nonuniform a new phenomenon becomes possible: a triplet component of the condensate wave function f (generally speaking, the condensate wave function is a matrix in the particle-hole and spin space) arises in the SF system.[3] This triplet component is an odd function of the Matsubara frequency ω (while the conventional BCS singlet component of f is an even function of ω) and spreads in the ferromagnet over a long distance of the order of $\xi_T = \sqrt{D/2\pi T}$. The existence of this long-range triplet odd-frequency component in SF structures with an inhomogeneous magnetization was predicted in Ref. 11 and further discussed in Ref. 12. Unlike the triplet component in

superfluid ^{3}He and in Sr$_2$RuO$_4$, this odd-frequency triplet component corresponds to s-wave pairing and, hence, is symmetric in the momentum space. Therefore it is not destroyed by scattering on nonmagnetic impurities and survives in the dirty limit. We call this component the long-range triplet component (LRTC). Historically, the odd-frequency triplet pairing was conjectured in 1974 by Berezinskii[13] as a possible mechanism for superfluidity in ^{3}He but this conjecture was not confirmed experimentally.

There is a significant amount of experimental data that may be interpreted as manifestation of the LRTC in SF systems.[14–22] Of particular importance are the experiments on SFS systems in which a long-range phase coherence of the condensate wave functions was observed in ferromagnets with a length considerably exceeding the penetration length of the singlet component ξ_h.[18,21,22] In principle, this long-range phase coherence can be due to the LRTC but, for unambiguous identification of the LRTC, further experimental and theoretical studies are very important. In particular, the theory of the LRTC was developed for specific types of the inhomogeneous magnetization in ferromagnets, which do not exhaust all possible types of the magnetic structures in real samples.

In Refs. 11, 12, and 23 the LRTC was studied in SF systems with a Bloch-type magnetic structure [the magnetization vector **M**(x) lies in the y-z plane parallel to the SF interface and rotates with increasing x]. The amplitude and the penetration length of the LRTC induced in the ferromagnet have been calculated in Refs. 11 and 23. Under certain conditions the LRTC penetrates the ferromagnet over a long distance of order ξ_T. As shown in Ref. 23, where a SFS structure with a conical ferromagnet was studied, the LRTC may decay in a nonmonotonic way provided the cone angle exceeds a certain value. In Refs. 24 and 25 a multilayered SF structure was investigated in which the magnetization vector **M**(x) has fixed but different orientations in different ferromagnetic layers. This structure is also similar to a Bloch-type domain structure.

At the same time, it is well known that the domain structure in a ferromagnet can be not only of the Bloch type but also of the Néel type.[26] A SF system with a Néel-type magnetic spiral structure [the $\mathbf{M}(y)$ vector lies in the $y-z$ plane parallel to the SF interface and rotates with increasing y] was studied theoretically in Ref. [27]. This magnetic structure may be regarded as an infinite Néel wall. It was shown that in this case the LRTC does not arise in the system. However, this statement is valid only for the case of a uniformly rotating $\mathbf{M}(y)$ vector. In a more realistic situation of a ferromagnet with magnetic domains separated by Néel walls, the LRTC arises at the domain walls and decays inside the domains over a long distance.[28] Another source of the triplet component in SF structures was considered in Ref. [29], where the SF interface was assumed to be spin-active. The Josephson effect in a S/HM/S junction (HM is a ferromagnetic half-metal) was studied in this paper and it was shown that the critical Josephson current has a maximum at low, but nonzero, temperature.

In the present paper we consider a SFS Josephson junction with the Néel domain structure in the ferromagnetic layer and calculate the Josephson critical current I_c in this system. Up to now there have been no theoretical investigations of this problem. In Refs. [30], [24], [25], and [23] the critical current I_c was calculated for a magnetic structure similar to the Bloch type. A SFS Josephson junction with a rotating $\mathbf{M}(x)$ and with the thickness of the F film d of order ξ_h was studied in Ref. [30]. It was shown that the rotation of the magnetization vector $\mathbf{M}(x)$ leads to the appearance of the LRTC and to a suppression of the π state in the Josephson junction. The situation in a multilayered SF structure with noncollinear magnetizations in the F layers is more complicated. The sign of I_c depends on the chirality, that is, on whether the $\mathbf{M}$ vector rotates in the same direction in the whole system or it oscillates with respect to the z axis.[24,25] In a SFS junction with a conical ferromagnet of thickness d much greater than ξ_h, the critical current I_c is due to the LRTC and the sign of I_c depends on the cone angle.[23]

Note that in ferromagnets with a multidomain structure the LRTC does not arise if the thickness of the domain walls is very small. In this case the magnetization vectors $\mathbf{M}$ are collinear and only singlet and short-range triplet components are induced due to the proximity effect. The critical current in a SFS junction with such a structure was calculated in Ref. [31]. The domain structure also results in a suppression of the π state due to an effective averaging of the exchange field. Moreover, if the exchange field $\mathbf{h}$ changes its sign over a scale shorter than $\max(\xi_h, l)$ (where l is the mean free path), long-range effects arise even in the absence of the LRTC (the exchange field is effectively averaged out). This case is realized provided an antiferromagnet (AF) is used in SFS junctions instead of a ferromagnet. The Josephson current in S/AF/S junctions was studied theoretically in Refs. [32] and [33] and experimentally (see Ref. [34], and references therein).

We consider a domain structure in a thin F film, where domains with antiparallel in-plane magnetizations are separated by the Néel walls (while the magnetization does not change across the thin F film). This domain structure is re-

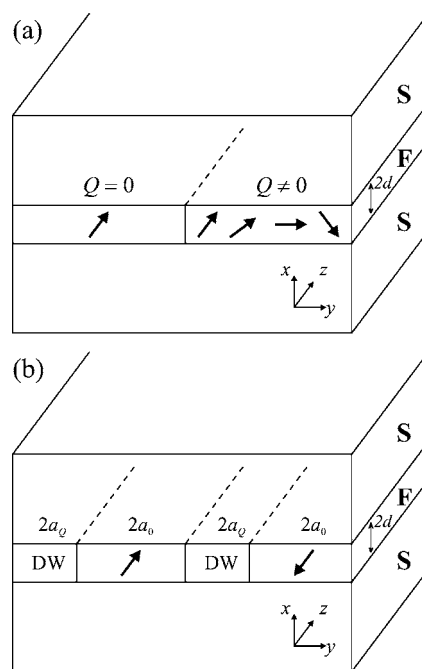
FIG. 1. SFS junctions considered in the paper. (a) The domain ($y<0$) and the region with rotating magnetization ($y>0$) in the F layer are half-infinite. (b) Multidomain F layer. Depending on the relative orientation of rotating magnetizations in the neighboring domain walls, we distinguish the cases of positive and negative chirality (Q has the same or opposite sign in the neighboring domain walls, respectively).

alized in real ferromagnetic films.[26] The y-z plane is chosen to be parallel to the SF interfaces (see Fig. 1). We show that the LRTC arises at the Néel domain walls and decays exponentially away from the domain walls and the SF interfaces over a long distance ξ_T. We calculate the Josephson current due to the LRTC and find that its sign corresponds to the π junction. The mechanism of the π junction in our case is related to $\pi/2$ phase shifts at the SF interfaces, while the LRTC does not oscillate inside the F layer (in contrast to the short-range component). We also study modifications of the density of states in the F film due to the LRTC.

The paper is organized as follows. In Sec. II, we formulate the Usadel equations and the corresponding boundary conditions, investigate the main features of the long-range triplet superconducting component that appears due to the presence of Néel domain walls, and find the Josephson current due to this component. The analysis is made for the simplified model with only one half-infinite region with rotating magnetization. In Sec. III, we consider the realistic case of the multidomain F layer using the results of Sec. II. In Sec. IV, we study the correction to the density of states due to the triplet component. This section is an addition to our previous paper Ref. [28]. Finally, we discuss limitations of our model in Sec. V and present our conclusions in Sec. VI.

II. BASIC EQUATIONS. JOSEPHSON EFFECT IN THE CASE OF A HALF-INFINITE DOMAIN

We consider a ferromagnet ($0<x<2d$) sandwiched between two bulk superconductors. We assume that the in-

plane exchange field $\mathbf{h}(y)$ in the F layer proportional to the magnetization $\mathbf{M}$, depends on y as follows: $\mathbf{h}(y) = h(0,0,1)$ at $y < 0$ and $\mathbf{h}(y) = h(0, \sin \alpha(y), \cos \alpha(y))$ with $\alpha(y) = Qy$ at $y > 0$. This means that the magnetization vector $\mathbf{M}$ is oriented along the z axis at $y < 0$ and rotates in the y-z plane at $y > 0$. The region with the rotating magnetization models the Néel domain wall. This structure is shown in Fig. 1(a) and contains only one half-infinite domain and one half-infinite region with rotating magnetization. Then we shall use the obtained results to describe a realistic multidomain structure depicted in Fig. 1(b).

In order to calculate the Josephson current, we need to find the condensate Green functions in the ferromagnet induced due to the proximity effect. We consider the dirty limit, which means, in particular, that $h\tau \ll 1$, where τ is the momentum relaxation time due to elastic scattering.

In the dirty limit, the system is described by the Usadel equation for the matrix Green function $\check{g}$ which is a 4×4 matrix in the Gor'kov-Nambu and spin spaces. The Usadel equation for the case of an inhomogeneous magnetization was written in Refs. 35 and 3. However, we redefine the Green function used in Refs. 35 and 3 (and also in our previous paper Ref. 28) introducing a new matrix function $\check{g}_{\mathrm{new}} = \check{V}\check{g}\check{V}^\dagger$ with the transformation matrix

$$\check{V} = \exp\left(i\frac{\pi}{4}(\hat{\tau}_3 - \hat{\tau}_0)\hat{\sigma}_3\right), \qquad (1)$$

where $\hat{\tau}_i$ and $\hat{\sigma}_i$ are the Pauli matrices in the Gor'kov-Nambu and spin spaces, respectively. This transformation was proposed in Ref. 36, and below we shall use the new Green function $\check{g}_{\mathrm{new}}$ omitting the subscript for brevity. The convenience of the new definition is that the Usadel equation for the new Green function possesses the explicit symmetry with respect to rotations of the exchange field $\mathbf{h}$:

$$D\,\boldsymbol{\nabla}\,(\check{g}\,\boldsymbol{\nabla}\,\check{g}) - \omega[\hat{\tau}_3\hat{\sigma}_0, \check{g}] - i[\hat{\tau}_3(\mathbf{h}\hat{\boldsymbol{\sigma}}), \check{g}] - [\check{\Delta}, \check{g}] = 0, \quad (2)$$

$$\check{\Delta} = (\hat{\tau}_1\mathrm{Re}\Delta - \hat{\tau}_2\,\mathrm{Im}\,\Delta)\hat{\sigma}_0,$$

where ω is the Matsubara frequency, $\mathbf{h} = h\mathbf{n}$, $\mathbf{n} = (0, \sin \alpha(y), \cos \alpha(y))$, and $\alpha(y) = 0$ at $y < 0$ while $\alpha(y) = Qy$ at $y > 0$. We assume that the diffusion coefficients D for electrons with spins up and down are equal to each other (this is correct provided the exchange energy h is much less than the Fermi energy ε_F).

The Usadel equation (2) is written in the general form taking into account both the superconductivity and magnetism. In the SFS junction, the pair potential Δ is nonzero only in the S layers, while the exchange field $\mathbf{h}$ is nonzero only in the F layer. There is no attractive interaction between electrons in the F layer, hence $\Delta = 0$. However, the condensate (Gor'kov) functions are finite in the F region due to the boundary conditions at the SF interface.

In the general case, the Green function has the following components

$$\check{g} = \hat{\tau}_3(\check{g}_0\hat{\sigma}_0 + \mathbf{g}\hat{\boldsymbol{\sigma}}) + \hat{\tau}_1(f_0\hat{\sigma}_0 + \mathbf{f}\hat{\boldsymbol{\sigma}}) + \hat{\tau}_2(\bar{f}_0\hat{\sigma}_0 + \bar{\mathbf{f}}\hat{\boldsymbol{\sigma}}). \quad (3)$$

In the bulk of a normal metal, only the g_0 component is present. The superconducting correlations are described by the scalar anomalous components f_0 and $\bar{f}_0$, while the vector components $(\mathbf{g}, \mathbf{f}, \bar{\mathbf{f}})$ are due to the ferromagnetism.

The superconducting correlations described by the f components (nondiagonal in the Nambu-Gor'kov space) are assumed to be weak due to a finite interface transparency. In the considered case of weak proximity effect ($|f| \ll 1$), the Green function acquires the form

$$\check{g} = \hat{\tau}_3\hat{\sigma}_0\,\mathrm{sgn}\,\omega + \check{F}, \qquad (4)$$

where the anomalous part can be written as

$$\check{F} = \hat{\tau}_1\hat{f} + \hat{\tau}_2\hat{\bar{f}} \qquad (5)$$

with matrices in the spin space

$$\hat{f} = f_0\hat{\sigma}_0 + \mathbf{f}\hat{\boldsymbol{\sigma}}, \qquad (6)$$

$$\hat{\bar{f}} = \bar{f}_0\hat{\sigma}_0 + \bar{\mathbf{f}}\hat{\boldsymbol{\sigma}}. \qquad (7)$$

Equation (2) can be linearized and brought to the form

$$\nabla^2\check{F} - 2k_\omega^2\check{F} - ik_h^2\,\mathrm{sgn}\,\omega\{\hat{\tau}_0(\mathbf{n}\hat{\boldsymbol{\sigma}}), \check{F}\} = 0, \qquad (8)$$

where $\omega = \pi T(2n+1)$, $k_\omega^2 = |\omega|/D$, $k_h^2 = h/D$, and the braces denote the anticommutator.

The anomalous part of the Green function in the bulk of the superconductor with the superconducting phase φ is $\check{F}_S(\varphi) = (\hat{\tau}_1 \cos \varphi - \hat{\tau}_2 \sin \varphi)\hat{\sigma}_0 f_S$, where

$$f_S = \frac{\Delta}{\sqrt{\omega^2 + \Delta^2}}. \qquad (9)$$

We intend to find the Josephson current at the phase difference φ between the two superconducting banks. Assuming the phases of the left and right superconductors to be $-\varphi/2$ and $\varphi/2$, respectively, we write the boundary conditions for $\check{F}$ at the SF interfaces

$$\frac{\partial\check{F}}{\partial x} = \mp\frac{\check{F}_S(\mp\varphi/2)}{\gamma_b}, \qquad (10)$$

where the two signs correspond to the left ($x=0$) and right ($x=2d$) SF interfaces, respectively. Here $\gamma_b = R_b\sigma$, while R_b is the interface resistance per unit area and σ is the conductivity of the ferromagnet. This boundary condition follows from the Kupriyanov-Lukichev ones[37] provided two assumptions are satisfied: (1) the proximity effect is weak (i.e., $\gamma_b/\xi_h \gg 1$) and (2) the bulk solution $\check{F}_S$ in the superconductors is unperturbed and valid up to the interface (i.e., $\gamma_b/\xi_S \gg \sigma/\sigma_S$, where $\xi_S = \sqrt{D_S/\Delta}$ and σ_S are the coherence length and the conductivity in the S banks).

The technical problem with Eq. (8) is that this is a two-dimensional partial-derivative differential equation. However, we can employ a trick similar to the one proposed in Ref. 28, which allows us to make the Fourier transformation

over x, reducing the problem to only one dimension y.

The equations for the $\hat{f}$ and $\hat{\bar{f}}$ functions split and for the $\hat{f}$ function we obtain

$$\nabla^2 \hat{f} - 2k_\omega^2 \hat{f} - ik_h^2 \, \mathrm{sgn}\, \omega\{(\mathbf{n}\hat{\boldsymbol{\sigma}}), \hat{f}\} = 0, \tag{11}$$

$$\left. \frac{\partial \hat{f}}{\partial x} \right|_{x=0,2d} = \mp \frac{f_S \cos \frac{\varphi}{2}}{\gamma_b} \hat{\sigma}_0. \tag{12}$$

The $\hat{\bar{f}}$ function obeys the same equation, although the boundary conditions are different

$$\nabla^2 \hat{\bar{f}} - 2k_\omega^2 \hat{\bar{f}} - ik_h^2 \, \mathrm{sgn}\, \omega\{(\mathbf{n}\hat{\boldsymbol{\sigma}}), \hat{\bar{f}}\} = 0, \tag{13}$$

$$\left. \frac{\partial \hat{\bar{f}}}{\partial x} \right|_{x=0,2d} = - \frac{f_S \sin \frac{\varphi}{2}}{\gamma_b} \hat{\sigma}_0. \tag{14}$$

The functions $\hat{f}$ and $\hat{\bar{f}}$ are defined for $0 \leq x \leq 2d$. The function $\hat{f}$ is even with respect to the center of the F layer, while $\hat{\bar{f}}$ is odd. We can continue the functions to the whole x axis: for $\hat{f}$ we do it periodically and for $\hat{\bar{f}}$—antiperiodically, obtaining continuous functions in both cases. Due to the boundary conditions both the functions have cusps at $x=2dN$ with integer N. The boundary conditions (10) producing the cusps can be incorporated into Eq. (8) itself as δ-functional terms (this situation is similar to the standard quantum-mechanical problem with δ-functional potential producing a cusp of the wave function):

$$\nabla^2 \hat{f} - 2k_\omega^2 \hat{f} - ik_h^2 \, \mathrm{sgn}\, \omega\{(\mathbf{n}\hat{\boldsymbol{\sigma}}), \hat{f}\}$$

$$= -\hat{\sigma}_0 \frac{2f_S \cos \frac{\varphi}{2}}{\gamma_b} \sum_{N=-\infty}^{\infty} \delta(x - 2dN), \tag{15}$$

$$\nabla^2 \hat{\bar{f}} - 2k_\omega^2 \hat{\bar{f}} - ik_h^2 \, \mathrm{sgn}\, \omega\{(\mathbf{n}\hat{\boldsymbol{\sigma}}), \hat{\bar{f}}\}$$

$$= -\hat{\sigma}_0 \frac{2f_S \sin \frac{\varphi}{2}}{\gamma_b} \sum_{N=-\infty}^{\infty} (-1)^N \delta(x - 2dN). \tag{16}$$

Now, instead of solving Eq. (8) at $0 \leq x \leq 2d$ with the boundary conditions (10), we have to solve Eqs. (15) and (16) at all x.

The Fourier transformation

$$f(k,y) = \int_{-d}^{d} dx \exp(-ikx) f(x,y) \tag{17}$$

in Eqs. (15) and (16) should be performed over "bosonic" wave vectors k_n and "fermionic" wave vectors $\bar{k}_n$ for the periodic function $\hat{f}$ and antiperiodic function $\hat{\bar{f}}$, respectively,

$$k_n = \frac{\pi}{2d} 2n, \quad \bar{k}_n = \frac{\pi}{2d} (2n+1). \tag{18}$$

We obtain

$$\frac{\partial^2 \hat{f}}{\partial y^2} - (k_n^2 + 2k_\omega^2) \hat{f} - ik_h^2 \, \mathrm{sgn}\, \omega\{(\mathbf{n}\hat{\boldsymbol{\sigma}}), \hat{f}\} = - \frac{2f_S \cos \frac{\varphi}{2}}{\gamma_b} \hat{\sigma}_0, \tag{19}$$

$$\frac{\partial^2 \hat{\bar{f}}}{\partial y^2} - (\bar{k}_n^2 + 2k_\omega^2) \hat{\bar{f}} - ik_h^2 \, \mathrm{sgn}\, \omega\{(\mathbf{n}\hat{\boldsymbol{\sigma}}), \hat{\bar{f}}\} = - \frac{2f_S \sin \frac{\varphi}{2}}{\gamma_b} \hat{\sigma}_0. \tag{20}$$

The two equations are similar and we may consider only one of them, say Eq. (19) for the $\hat{f}$ function. Then the result for the $\hat{\bar{f}}$ function can immediately be obtained by substituting $k_n \mapsto \bar{k}_n$ and $\cos \frac{\varphi}{2} \mapsto \sin \frac{\varphi}{2}$.

At $y>0$ the function $\alpha(y)$ is y dependent, while at $y<0$ we have $\alpha=0$. In the region of positive y one can exclude the y dependence from Eq. (19) with the help of a rotation

$$\hat{f} = \hat{U} \hat{f}_u \hat{U}^+, \tag{21}$$

where $\hat{U} = \exp[i\hat{\sigma}_1 \alpha(y)/2]$. As a result, we get $(y>0)$

$$\frac{\partial^2 \hat{f}_u}{\partial y^2} - \left(k_n^2 + \frac{Q^2}{2} + 2k_\omega^2 \right) \hat{f}_u + \frac{Q^2}{2} \hat{\sigma}_1 \hat{f}_u \hat{\sigma}_1 + iQ \left[\hat{\sigma}_1, \frac{\partial \hat{f}_u}{\partial y} \right]$$

$$- ik_h^2 \, \mathrm{sgn}\, \omega\{\hat{\sigma}_3, \hat{f}_u\} = - \frac{2f_S \cos \frac{\varphi}{2}}{\gamma_b} \hat{\sigma}_0 \tag{22}$$

in terms of the new function $\hat{f}_u(k,y)$ (the square brackets denote the commutator). The same equation is valid for $y<0$ if we put $Q=0$

$$\frac{\partial^2 \hat{f}_u}{\partial y^2} - (k_n^2 + 2k_\omega^2) \hat{f}_u - ik_h^2 \, \mathrm{sgn}\, \omega\{\hat{\sigma}_3, \hat{f}_u\} = - \frac{2f_S \cos \frac{\varphi}{2}}{\gamma_b} \hat{\sigma}_0. \tag{23}$$

The original functions $\hat{f}$ and $\partial \hat{f}/\partial y$ are continuous at $y=0$. Therefore, the rotated functions obey the following boundary conditions at $y=0$:

$$\hat{f}_u(-0) = \hat{f}_u(+0), \tag{24}$$

$$\frac{\partial \hat{f}_u(-0)}{\partial y} = \frac{\partial \hat{f}_u(+0)}{\partial y} + i\frac{Q}{2}[\hat{\sigma}_1, \hat{f}_u]. \tag{25}$$

Thus, we have to solve the linear matrix Eqs. (22) $(y>0)$ and (23) $(y<0)$ of the second order with the boundary conditions (24) and (25) at $y=0$. We can represent the solution in the form

$$\hat{f}_u = \hat{\mathcal{F}}(Q)\theta(y) + \hat{\mathcal{F}}(0)\theta(-y) + \delta\hat{f}_u, \tag{26}$$

where θ is the Heaviside step function and the constants $\hat{\mathcal{F}}(Q)$ and $\hat{\mathcal{F}}(0)$ are the homogeneous solutions of Eqs. (22) and (23) at $y = \pm\infty$. The matrices $\hat{\mathcal{F}}$ have the form

$$\hat{\mathcal{F}} = \hat{\sigma}_0\mathcal{F}_0 + \hat{\sigma}_3\mathcal{F}_3, \tag{27}$$

where

$$\mathcal{F}_0(Q) = \frac{2f_S\cos\dfrac{\varphi}{2}(k_n^2 + Q^2 + 2k_\omega^2)}{\gamma_b\mathcal{D}(Q)}, \tag{28}$$

$$\mathcal{F}_3(Q) = -\frac{4if_S\cos\dfrac{\varphi}{2}k_h^2\,\mathrm{sgn}\,\omega}{\gamma_b\mathcal{D}(Q)}, \tag{29}$$

and

$$\mathcal{D}(Q) = (k_n^2 + Q^2 + 2k_\omega^2)(k_n^2 + 2k_\omega^2) + 4k_h^4. \tag{30}$$

The correction $\delta\hat{f}_u(k, y)$ obeys the same Eqs. (22) and (23) without the right-hand side. It has the form

$$\delta\hat{f}_u = \hat{\sigma}_0 f_0 + \hat{\sigma}_3 f_3 + \hat{\sigma}_2 f_2. \tag{31}$$

The first term in Eq. (31) is the singlet component. The second term is the triplet component with zero z projection of the Cooper-pair spin. This component arises even in the case of a homogenous magnetization of the ferromagnet and decays in the F film at the short distance ξ_h. The last term in Eq. (31) is the triplet component with the spin projection ± 1. It arises in the case of an inhomogeneous magnetization and decays over a long distance of the order ξ_T. The functions $f_i(k, y)$ in Eq. (31) can be represented as a sum of eigenfunctions of Eqs. (22) and (23), i.e.,

$$f_i(y) = \sum_l A_{il}\exp[-\kappa_l(Q)y] \quad \text{at } y > 0, \tag{32}$$

$$f_i(y) = \sum_l B_{il}\exp[\kappa_l(0)y] \quad \text{at } y < 0. \tag{33}$$

The inverse decay lengths $\kappa_l(Q)$ are the eigenvalues of Eqs. (22) and (23) (without the right-hand side). The equation for $\kappa_l(Q)$ has the form ($l = 1, 2, 3$)

$$[(\kappa_l^2 - k_n^2 - Q^2 - 2k_\omega^2)^2 + 4(Q\kappa_l)^2](\kappa_l^2 - k_n^2 - 2k_\omega^2) + 4k_h^4(\kappa_l^2 - k_n^2 - Q^2 - 2k_\omega^2) = 0. \tag{34}$$

We assume that the exchange length is the shortest length in the problem

$$k_h^2 \gg k_n^2, Q^2, k_\omega^2. \tag{35}$$

Then, the eigenvalues κ_l consist of two "short-range" values

$$\kappa_\pm \approx (1 \mp i\,\mathrm{sgn}\,\omega)k_h \tag{36}$$

and one "long-range" value

$$\kappa_L(Q) \approx \sqrt{k_n^2 + Q^2 + 2k_\omega^2}. \tag{37}$$

At $y < 0$ we have the same κ_l with $Q = 0$.

Calculating the corresponding eigenvectors and matching solutions (32) and (33) with the help of the boundary conditions (24) and (25), we find the coefficients A_{il} and B_{il}. This simple but cumbersome calculation is similar to the one presented in Ref. 28. In the considered limit of a small exchange length [see Eq. (35)], the coefficients A_{2L} and B_{2L} that describe the LRTC are the largest ones

$$A_{2L} \approx B_{2L} \approx \frac{Q\mathcal{F}_3}{\kappa_Q + \kappa_0}, \tag{38}$$

where for brevity we have denoted

$$\kappa_Q \equiv \kappa_L(Q), \quad \kappa_0 \equiv \kappa_L(0). \tag{39}$$

In the limit (35) the function $\mathcal{F}_3(Q)$ has a simple form

$$\mathcal{F}_3 \approx -\frac{if_S\cos\dfrac{\varphi}{2}\,\mathrm{sgn}\,\omega}{\gamma_b k_h^2}. \tag{40}$$

Therefore, the magnitude of the LRTC at the interface between the domain and the domain wall ($y = 0$) is equal to

$$f_L(k_n, 0) \equiv f_{2L}(k_n, 0) = -\frac{if_S\cos\dfrac{\varphi}{2}\,\mathrm{sgn}\,\omega}{\gamma_b k_h^2}\frac{Q}{\kappa_Q + \kappa_0}, \tag{41}$$

while the decay along the y axis is determined by κ_0 or κ_Q at $y < 0$ and $y > 0$, respectively [see Eq. (32)]. Below we consider the situations when only the LRTC is essential, and denote the corresponding contribution f_{2L} to the Green function by f_L for brevity.

The real-space function is determined by the inverse Fourier transform

$$f_L(x, y) = \frac{1}{2d}\sum_{k_n} e^{ik_n x}f_L(k_n, y). \tag{42}$$

The $\bar{f}_L$ function is obtained after substituting $k_n \mapsto \bar{k}_n$ and $\cos\frac{\varphi}{2} \mapsto \sin\frac{\varphi}{2}$.

Josephson current. The supercurrent density is determined by the anomalous part of the Green function

$$\mathbf{j} = \frac{i\sigma\pi T}{4e}\mathrm{Tr}\sum_\omega \hat{\tau}_3\hat{\sigma}_0\check{F}\,\boldsymbol{\nabla}\,\check{F}, \tag{43}$$

where σ is the conductivity in the normal state (we shall calculate this expression inside the F layer, hence σ is the conductivity of the F material). Since we choose the phases of the left and right superconductor as $\mp\varphi/2$, then the f components are even with respect to the center of the interlayer, while the $\bar{f}$ components are odd. Calculating the supercurrent in the center of the F layer, we obtain

$$\mathrm{Tr}(\hat{\tau}_3\hat{\sigma}_0\check{F}\,\boldsymbol{\nabla}\,\check{F}) = 4i(f_0\,\boldsymbol{\nabla}\,\bar{f}_0 + \mathbf{f}\,\boldsymbol{\nabla}\,\bar{\mathbf{f}}). \tag{44}$$

Only the x component of the current survives due to the odd behavior of the $\bar{f}$ functions.

However, calculating the current not in the center of the F layer we also obtain the y component. In the region of the F layer, where only the long-range component is present, we have $\check{F} = \hat{\tau}_1 \hat{\sigma}_2 f_L + \hat{\tau}_2 \hat{\sigma}_2 \bar{f}_L$ and finally

$$\mathbf{j} = \frac{\sigma \pi T}{e} \sum_{\omega} (\bar{f}_L \boldsymbol{\nabla} f_L - f_L \boldsymbol{\nabla} \bar{f}_L). \tag{45}$$

In the region with the magnetization rotating as a function of y, the final expression remains the same with f_L and $\bar{f}_L$ being the second components of $\hat{f}_u$, see Eqs. (21), (26), and (31).

Inside the half-infinite domain, Eq. (42) immediately yields

$$f_L(x,y) = -\sum_{k_n} e^{ik_n x} \frac{if_S \cos(\varphi/2) Q \operatorname{sgn} \omega}{2d\gamma_b k_h^2 (\kappa_Q + \kappa_0)} e^{\kappa_0 y}, \tag{46}$$

$$\bar{f}_L(x,y) = -\sum_{\bar{k}_n} e^{i\bar{k}_n x} \frac{if_S \sin(\varphi/2) Q \operatorname{sgn} \omega}{2d\gamma_b k_h^2 (\kappa_Q + \kappa_0)} e^{\kappa_0 y}. \tag{47}$$

In the limit of thin F layer, i.e., $d \ll 1/Q, 1/k_\omega$ (at the same time, we assume $1/k_h \ll d$, which allows us to neglect the short-range components), we obtain

$$
\begin{aligned}
f_L(x,y) = {} & -\frac{if_S \cos(\varphi/2)\operatorname{sgn}\omega}{2d\gamma_b k_h^2} \\
& \times \left(\frac{Q}{\sqrt{Q^2 + 2k_\omega^2} + \sqrt{2}k_\omega} e^{\sqrt{2}k_\omega y} \right. \\
& \left. + \sum_{k_n > 0} \frac{Q}{k_n} \cos(k_n x) e^{k_n y} \right),
\end{aligned}
\tag{48}
$$

$$\bar{f}_L(x,y) = -\frac{if_S \sin(\varphi/2)\operatorname{sgn}\omega}{2d\gamma_b k_h^2} \sum_{\bar{k}_n > 0} \frac{Q}{\bar{k}_n} \cos(\bar{k}_n x) e^{\bar{k}_n y}. \tag{49}$$

We calculate the Josephson current according to Eq. (45). In the limit of thin F layer, the main contribution is given by the second term in the brackets $f_L \boldsymbol{\nabla} \bar{f}_L$, moreover, it is sufficient to keep only the $k_n = 0$ component in f_L [the first term in the brackets in Eq. (48)]. This is because the components containing k_n in the denominator in Eq. (48) are much smaller. Summing over $\bar{k}_n$ finally yields

$$
\begin{aligned}
\mathbf{j}(x,y) = {} & -\sin\varphi \frac{\sigma Q^2 \pi T}{16e(d\gamma_b k_h^2)^2} \\
& \times \sum_\omega \frac{f_S^2}{\sqrt{Q^2 + 2k_\omega^2} + \sqrt{2}k_\omega} \exp(-\sqrt{2}k_\omega|y|) \\
& \times \frac{\mathbf{e}_x \cosh\left(\dfrac{\pi y}{2d}\right)\sin\left(\dfrac{\pi x}{2d}\right) + \mathbf{e}_y \sinh\left(\dfrac{\pi y}{2d}\right)\cos\left(\dfrac{\pi x}{2d}\right)}{\sinh^2\left(\dfrac{\pi y}{2d}\right) + \sin^2\left(\dfrac{\pi x}{2d}\right)},
\end{aligned}
\tag{50}
$$

where $\mathbf{e}_x$ and $\mathbf{e}_y$ are the unit vectors in the x and y directions, respectively. In the region with $Q \neq 0$, we obtain Eq. (50)
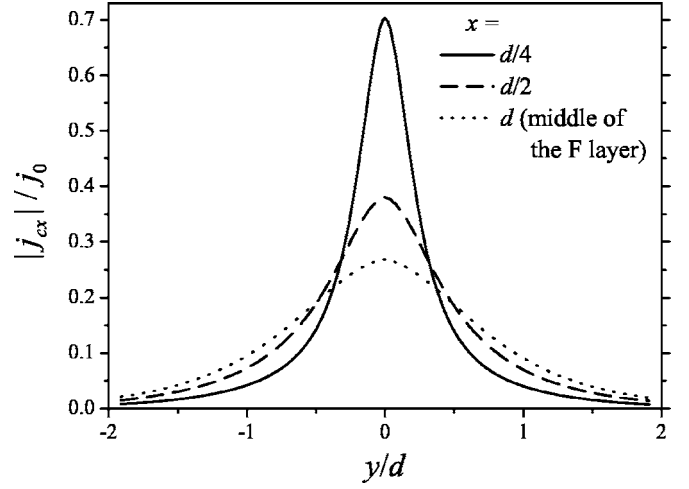

FIG. 2. SFS junction with a half-infinite domain: absolute value of the critical current density j_{cx} in the x direction as a function of the y coordinate at low temperatures. The current is negative, i.e., the π state of the junction is realized. The normalization constant is $j_0 = \sigma D Q^3 / 8e(d\gamma_b k_h^2)^2$. Other parameters: $DQ^2 = \Delta$ and $Qd = 0.1$.

with $\sqrt{Q^2 + 2k_\omega^2}$ instead of $\sqrt{2k_\omega^2}$ in the argument of the exponential. The main qualitative result of this formula is that the x component of the current density has a form $j_x = j_{cx} \sin\varphi$ with negative j_{cx}, i.e., the π state of the junction is realized.

Expression (50) for the supercurrent is valid in the region where only the LRTC component is essential, while the short-range components are exponentially small. Therefore, close to the SF interfaces and to the boundary between the domain and the domain wall (at distances of the order of ξ_h) the expression is not applicable.

Note that $\boldsymbol{\nabla}\mathbf{j} = 0$ and $\boldsymbol{\nabla}\times\mathbf{j} = 0$ within our accuracy (we must neglect k_ω and Q in comparison with $1/d$). The total y current is absent, while the total x current is equally shared between the regions with constant and rotating magnetization and corresponds to the π junction:

$$\int_0^{2d} j_y(x,y) dx = 0, \tag{51}$$

$$
\begin{aligned}
\int_{-\infty}^0 j_x(x,y) dy = {} & \int_0^\infty j_x(x,y) dy = -\sin\varphi \frac{\sigma Q^2 \pi T}{16ed\gamma_b^2 k_h^4} \\
& \times \sum_\omega \frac{f_S^2}{\sqrt{Q^2 + 2k_\omega^2} + \sqrt{2}k_\omega}.
\end{aligned}
\tag{52}
$$

The results for the x component of the critical current density $j_{cx}(x,y)$ are illustrated in Fig. 2, where we plot $|j_{cx}|$ as a function of y at several values of x. The current density is maximal at the boundary between the domain and the domain wall ($y = 0$), and the maximal current across the junction is carried along this line. At the same time, the relative height of this peak depends on x. The distribution is smoothest at the center of the F layer (i.e., at $x = d$), while the peak at the domain-domain-wall boundary becomes more pronounced closer to the SF interfaces.

In order to estimate the absolute value of the critical Josephson current following from Eq. (52), we assume that the junction area is 50×50 μm^2, $\sigma \sim (50$ $\mu\Omega$ cm$)^{-1}$, $Q \sim (50$ nm$)^{-1}$, $d \sim \gamma_b \sim 5\xi_h$, $h \sim 500$ K, and $D \sim 10$ cm^2/s. Then the critical current at low temperatures is of order 3 μA which is well within the experimentally measurable range.

III. JOSEPHSON EFFECT IN A MULTIDOMAIN SFS JUNCTION

In this section we study the LRTC in a SF structure with a multidomain ferromagnetic layer [Fig. 1(b)]. One can distinguish between two possibilities: (a) positive chirality, when the magnetization vector $\mathbf{M}(y)$ in all the domain walls rotates in the same direction (e.g., clockwise) and (b) negative chirality, when the vector $\mathbf{M}(y)$ in neighboring domain walls rotates in the opposite directions [e.g., clockwise in the $2n$th domain walls and counterclockwise in the $(2n+1)$th domain walls]. We are interested in the LRTC assuming that the exchange length ξ_h is much smaller than the coherence length ξ_T. At distances x essentially exceeding the length ξ_h only the LRTC survives in the F layer.

We assume that the width of the domains with $Q=0$ is $2a_0$ and the width of the domain walls ($Q \neq 0$) is $2a_Q$. The origin ($y=0$) is located in the middle of a domain with the constant magnetization. At $x \gg \xi_h$ only the long-range components of the condensate function survive in the ferromagnet. The largest long-range component is the LRTC. At the boundary between a domain and a domain wall the solution must satisfy boundary conditions (24) and (25).

A. Positive chirality

Consider first the case of positive chirality. The angle $\alpha(y)$ is then an odd function of y, which means that $f_2(y)$ is also odd—this general symmetry can be demonstrated in Eq. (15). Hence the solution for the LRTC is

$$f_L(k_n, y) = A \sinh(\kappa_0 y), \quad -a_0 < y < a_0, \tag{53}$$

$$f_L(k_n, y) = B \sinh[\kappa_Q(y - a_0 - a_Q)], \quad a_0 < y < a_0 + 2a_Q. \tag{54}$$

Matching these solutions and their derivatives at $y=a_0$, we find

$$B = -A \frac{\sinh(\kappa_0 a_0)}{\sinh(\kappa_Q a_Q)} = -\frac{Q\mathcal{F}_3}{\cosh(\kappa_Q a_Q)\left(\kappa_Q + \kappa_0 \frac{\tanh(\kappa_Q a_Q)}{\tanh(\kappa_0 a_0)}\right)}. \tag{55}$$

The amplitude of the LRTC at $y=a_0$ is

$$f_L(k_n, a_0) = \frac{Q\mathcal{F}_3}{\kappa_Q \coth(\kappa_Q a_Q) + \kappa_0 \coth(\kappa_0 a_0)}. \tag{56}$$

We see that $f_L(k_n, a_0)$ turns to zero both at $a_Q \to 0$ and $a_0 \to 0$. These limits mean that the widths of the domain walls and domains are assumed to be small in comparison

with ξ_T but larger than ξ_h. The case $a_Q=0$ implies that we have a domain structure with the collinear orientation of magnetizations. The case $a_0=0$ corresponds to a SF structure with continuously rotating magnetization (the case studied in Ref. 27). In both the cases, the LRTC does not arise.

The spatial dependence of the LRTC in the domain ($|y|<a_0$), corresponding to Eq. (56), is given by the inverse Fourier transformation

$$f_L(x,y) = \frac{1}{2d} \sum_{n=-\infty}^{\infty} e^{ik_n x} f_L(k_n, a_0) \frac{\sinh(\kappa_0 y)}{\sinh(\kappa_0 a_0)}. \tag{57}$$

Interestingly, the function $f_L(x,y)$ turns to zero in the center of the domain ($y=0$). This means that the Josephson current due to the LRTC also turns to zero in the domain center.

Formula (57) can be drastically simplified in the limit when the F film is thin for the long-range component but thick for the short-range one (i.e., $k_h \gg 1/d \gg Q, k_\omega$). In this case, the main contribution is given by the $n=0$ harmonic (with $k_n=0$), since otherwise κ_Q and κ_0 in the denominator of Eq. (56) become very large. Employing also Eq. (40) we therefore obtain

$$f_L(y) = -\frac{if_S \cos(\varphi/2)\text{sgn }\omega}{2d\gamma_b k_h^2} \frac{Q}{\mathcal{K}_+} \frac{\sinh(\sqrt{2}k_\omega y)}{\sinh(\sqrt{2}k_\omega a_0)}, \tag{58}$$

where we have denoted

$$\mathcal{K}_+ = \sqrt{Q^2 + 2k_\omega^2} \coth(\sqrt{Q^2 + 2k_\omega^2} a_Q) + \sqrt{2}k_\omega \coth(\sqrt{2}k_\omega a_0). \tag{59}$$

The x dependence has vanished since the F layer is thin and the even function $f_L(x)$ is nearly constant.

Now we can easily write down the result for $\bar{f}_L$, employing the rule formulated in Sec. II: in Eq. (57) we should substitute $k_n \mapsto \bar{k}_n$ and $\cos\frac{\varphi}{2} \mapsto \sin\frac{\varphi}{2}$. After that we make the final step, assuming the limit of thin F layer. This step is different from the case of the f_L function, because there is no mode with $\bar{k}_n=0$, hence we must retain all the modes in the sum over n:

$$\bar{f}_L(x,y) = -\frac{if_S \sin(\varphi/2)\text{sgn }\omega}{2d\gamma_b k_h^2}$$

$$\times \sum_{\bar{k}_n > 0} \frac{2Q \cos \bar{k}_n x}{\bar{k}_n[\coth(\bar{k}_n a_Q) + \coth(\bar{k}_n a_0)]} \frac{\sinh(\bar{k}_n y)}{\sinh(\bar{k}_n a_0)}. \tag{60}$$

Finally, we find the supercurrent

$$\mathbf{j}_0(x,y) = -\sin\varphi \frac{\sigma Q^2 \pi T}{4e(d\gamma_b k_h^2)^2} \sum_\omega \frac{f_S^2}{\mathcal{K}_+} \frac{\sinh(\sqrt{2}k_\omega y)}{\sinh(\sqrt{2}k_\omega a_0)}$$

$$\times \sum_{\bar{k}_n > 0} \frac{\mathbf{e}_x \sin(\bar{k}_n x)\sinh(\bar{k}_n y) - \mathbf{e}_y \cos(\bar{k}_n x)\cosh(\bar{k}_n y)}{[\coth(\bar{k}_n a_Q) + \coth(\bar{k}_n a_0)]\sinh(\bar{k}_n a_0)}. \tag{61}$$

If we want to calculate the current in the region with $Q \neq 0$,

then we obtain the same expression, but with y counted from the center of the domain wall, with $\sqrt{Q^2 + 2k_\omega^2}$ instead of $\sqrt{2k_\omega^2}$ in the arguments of two sinh's, and with a_Q instead of a_0 in the arguments of two sinh's. For example, at $a_0 < y < a_0 + 2a_Q$, we have

$$\mathbf{j}_Q(x,y) = -\sin\varphi \frac{\sigma Q^2 \pi T}{4e(d\gamma_b k_h^2)^2} \sum_\omega \frac{f_S^2 \sinh(\sqrt{Q^2 + 2k_\omega^2}\,y')}{\mathcal{K}_+ \sinh(\sqrt{Q^2 + 2k_\omega^2}\,a_Q)}$$
$$\times \sum_{\bar{k}_n > 0} \frac{\mathbf{e}_x \sin(\bar{k}_n x)\sinh(\bar{k}_n y') - \mathbf{e}_y \cos(\bar{k}_n x)\cosh(\bar{k}_n y')}{[\coth(\bar{k}_n a_Q) + \coth(\bar{k}_n a_0)]\sinh(\bar{k}_n a_Q)},$$
(62)

where $y' = y - a_Q - a_0$.

B. Negative chirality

Consider now the case of negative chirality, when the $\mathbf{M}(y)$ vector rotates in the opposite directions in neighboring domain walls. In this case the spatial dependence of $f_2(y)$ in the domain walls remains the same as before, i.e., this function is odd with respect to the center of a domain wall. However, the spatial dependence of the LRTC in the domains changes drastically: it becomes an even function with respect to the center of a domain. Therefore this dependence is

$$f_L(k_n, y) = C \cosh(\kappa_0 y), \quad -a_0 < y < a_0,$$
(63)

$$f_L(k_n, y) = D \sinh[\kappa_Q(y - a_0 - a_Q)], \quad a_0 < y < a_0 + 2a_Q.$$
(64)

From the boundary conditions (24) and (25) we find the coefficients C and D, and finally obtain

$$f_L(k_n, a_0) = \frac{Q\mathcal{F}_3}{\kappa_Q \coth(\kappa_Q a_Q) + \kappa_0 \tanh(\kappa_0 a_0)}.$$
(65)

In this case the LRTC disappears only in the limit $a_Q \to 0$ because in this limit one again has a domain structure with the collinear orientation of magnetizations and very narrow domain walls.

Further analysis is similar to that for the previous case of positive chirality. Inside of the domain ($|y| < a_0$) we obtain

$$f_L(x,y) = \frac{1}{2d} \sum_{k_n} e^{ik_n x} f_L(k_n, a_0) \frac{\cosh(\kappa_0 y)}{\cosh(\kappa_0 a_0)}.$$
(66)

In the limit $k_h \gg 1/d \gg Q, k_\omega$, Eq. (66) yields

$$f_L(y) = -\frac{i f_S \cos(\varphi/2)\text{sgn }\omega}{2d\gamma_b k_h^2} \frac{Q \cosh(\sqrt{2}k_\omega y)}{\mathcal{K}_- \cosh(\sqrt{2}k_\omega a_0)},$$
(67)

$$\bar{f}_L(x,y) = -\frac{i f_S \sin(\varphi/2)\text{sgn }\omega}{2d\gamma_b k_h^2}$$
$$\times \sum_{\bar{k}_n > 0} \frac{2Q \cos \bar{k}_n x}{\bar{k}_n[\coth(\bar{k}_n a_Q) + \tanh(\bar{k}_n a_0)]} \frac{\cosh(\bar{k}_n y)}{\cosh(\bar{k}_n a_0)},$$
(68)

where we have denoted

$$\mathcal{K}_- = \sqrt{Q^2 + 2k_\omega^2}\coth(\sqrt{Q^2 + 2k_\omega^2}\,a_Q) + \sqrt{2}k_\omega \tanh(\sqrt{2}k_\omega a_0).$$
(69)

Finally, we find the supercurrent

$$\mathbf{j}_0(x,y) = -\sin\varphi \frac{\sigma Q^2 \pi T}{4e(d\gamma_b k_h^2)^2} \sum_\omega \frac{f_S^2 \cosh(\sqrt{2}k_\omega y)}{\mathcal{K}_- \cosh(\sqrt{2}k_\omega a_0)}$$
$$\times \sum_{\bar{k}_n > 0} \frac{\mathbf{e}_x \sin(\bar{k}_n x)\cosh(\bar{k}_n y) - \mathbf{e}_y \cos(\bar{k}_n x)\sinh(\bar{k}_n y)}{[\coth(\bar{k}_n a_Q) + \tanh(\bar{k}_n a_0)]\cosh(\bar{k}_n a_0)}.$$
(70)

Similarly, in the region with $Q \neq 0$ (at $a_0 < y < a_0 + 2a_Q$), we obtain

$$\mathbf{j}_Q(x,y) = -\sin\varphi \frac{\sigma Q^2 \pi T}{4e(d\gamma_b k_h^2)^2} \sum_\omega \frac{f_S^2 \sinh(\sqrt{Q^2 + 2k_\omega^2}\,y')}{\mathcal{K}_- \sinh(\sqrt{Q^2 + 2k_\omega^2}\,a_Q)}$$
$$\times \sum_{\bar{k}_n > 0} \frac{\mathbf{e}_x \sin(\bar{k}_n x)\cosh(\bar{k}_n y') - \mathbf{e}_y \cos(\bar{k}_n x)\sinh(\bar{k}_n y')}{[\coth(\bar{k}_n a_Q) + \tanh(\bar{k}_n a_0)]\sinh(\bar{k}_n a_Q)},$$
(71)

where $y' = y - a_Q - a_0$.

C. Discussion of the results

The expressions obtained for the supercurrent are valid in the region where only the LRTC component is essential, while the short-range components are exponentially small. Therefore, close to the SF interfaces and to the boundaries between domains and domain walls (at distances of the order of ξ_h) the expressions are not applicable.

The main qualitative result of expressions (61), (62), (70), and (71) is that the x component of the current density has a form $j_x = j_{cx} \sin\varphi$ with negative j_{cx}, i.e., the π state of the junction is realized. The $j_x(x)$ function is even while $j_y(x)$ is odd with respect to $x = d$ (the center of the F layer) at both chiralities. The total current in the y direction is zero. Within our accuracy $\nabla \mathbf{j} = 0$ and $\nabla \times \mathbf{j} = 0$ (we must neglect k_ω and Q in comparison with $\bar{k}_n$).

The LRTC is generated at the boundaries between the domains and the domain walls. As a result, the maximal supercurrent in the x direction is carried along these lines.

Integrating the x component of the supercurrent over y, we find the critical current per period of the structure:[38]

$$J_{c+} \equiv \int_{-a_0-a_Q}^{a_0+a_Q} j_{cx+}(y)dy = -\frac{\sigma Q^2 \pi T}{4ed\gamma_b^2 k_h^4} \sum_\omega \frac{f_S^2}{\mathcal{K}_+},$$
(72)

$$J_{c-} \equiv \int_{-a_0-a_Q}^{a_0+a_Q} j_{cx-}(y)dy = -\frac{\sigma Q^2 \pi T}{4ed\gamma_b^2 k_h^4} \sum_\omega \frac{f_S^2}{\mathcal{K}_-},$$
(73)

in the cases of positive and negative chirality, respectively. The total current across a junction of large area is proportional to the number of domain walls.

The results for the critical current are illustrated in Fig. 3, where we plot $|J_{c+}|$ and $|J_{c-}|$ as functions of the domain half-
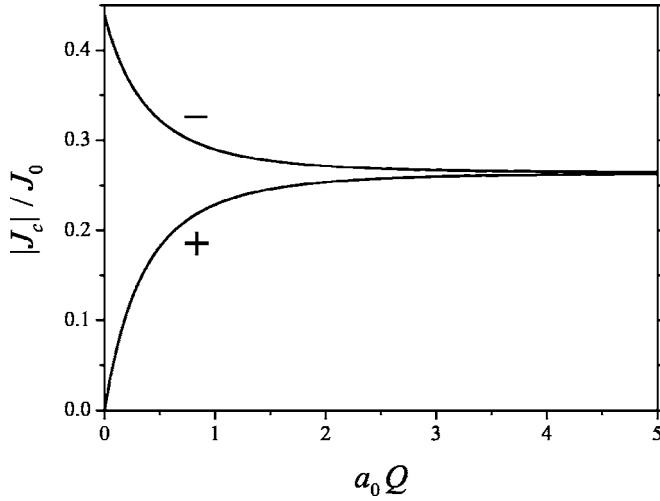
FIG. 3. Multidomain SFS junction: the absolute values of the critical currents J_{c+} (positive chirality) and J_{c-} (negative chirality) per period of the domain structure as functions of the domain half-width a_0 at low temperatures. The currents are negative, i.e., the π state of the junction is realized. The normalization constant is $J_0 = \sigma D Q^3 / 4 e d \gamma_b^2 k_h^4$. Other parameters: $DQ^2 = \Delta$ and the rotation of magnetization in the domain walls corresponds to $2 Q a_Q = \pi$.

width a_0 (while Q and a_Q are linked by the condition $2Qa_Q = \pi$ meaning rotation of the magnetization by the angle π in the domain wall). In the limit $a_0 \rightarrow 0$ the behavior of the supercurrent in the cases of positive and negative chiralities is drastically different. In the case of positive chirality, the LRTC disappears in this limit and the supercurrent vanishes,[39] while in the case of negative chirality this is the most inhomogeneous limit and the supercurrent is maximal. In the opposite limit of large $a_0 \gg \xi_T$, the a_0 dependence vanishes in both cases and the results coincide since the hyperbolic functions of $k_\omega a_0$ turn to unity.

The appearance of the π junction in SFS junctions is well understood in the case when it is due to the short-range component.[1] The key ingredient is the oscillating behavior of this component: the additional phase π across the junction is provided by changing the sign. At the same time, the LRTC does not change its sign, therefore the π junction due to the LRTC seems counterintuitive. Where does the additional phase come from? Note that the LRTC in our case is purely imaginary [see, e.g., Eq. (58)]. This means that there is a $\pi/2$ phase rotation at the SF interfaces, and the two interfaces provide the π shift. The mechanism of the π junction due to $\pi/2$ interface shifts is similar to Ref. 40.

Another type of SF structures, sensitive to the chirality of the vector **M**, was considered in Refs. 24 and 25. It was shown that the sign of the critical Josephson current in a multilayered SF structure depends on chirality. Similarly to the present paper, the π junction was found in the situation when only the LRTC is essential.

IV. DOS IN SF BILAYER

Our previous paper, Ref. 28, was devoted to studying the density of states (DOS) at the free surface of the F layer in
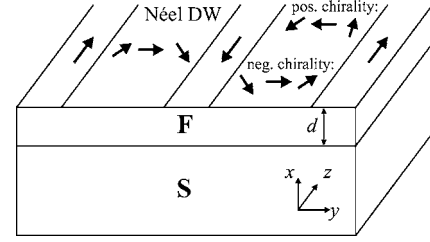

FIG. 4. Multidomain F layer of thickness d in contact with a bulk superconductor. Depending on the relative orientation of rotating magnetizations in neighboring domain walls, we distinguish the cases of positive and negative chirality (Q has the same or opposite sign in the neighboring domain walls, respectively). The proportion between the widths of domains and domain walls is chosen only for drawing purposes.

the system shown in Fig. 4 (with F layer of thickness d). These results are immediately reproduced from the Green function calculated in the center of the F layer in the SFS junction of Fig. 1(b) (with F layer of thickness $2d$) at zero phase difference, $\varphi = 0$. Making analytical continuation from the Matsubara frequency ω to the real energy ε, we obtain the correction to the DOS due to the proximity effect as

$$\delta\nu(\varepsilon) = -\left. \frac{\text{Re } f_L^2}{2} \right|_{\omega \rightarrow -i\varepsilon} \tag{74}$$

(we consider the region in space where only the LRTC is essential).

We want to return to this question in view of the recent paper,[41] where it was demonstrated that general analytical properties of the Green function imply that if the superconductivity has odd frequency symmetry, then $\delta\nu(0) > 0$. The expressions for the DOS from our paper Ref. 28 testify that this general statement is satisfied in our case, however, this fact was not illustrated in the figures. Figures 5 and 6
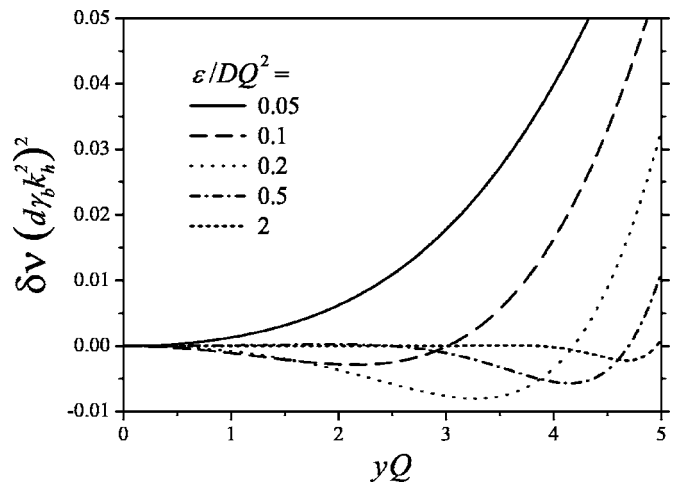

FIG. 5. Addition to Fig. 2 from Ref. 28: Correction $\delta\nu(y)$ (due to the proximity effect) to the DOS at the free surface of the F layer in the case of positive chirality. The curves are plotted at several energies ε. The width of the domains is $a_0 = 5/Q$, while the rotation of magnetization in the domain walls corresponds to $Q a_Q = \pi$.
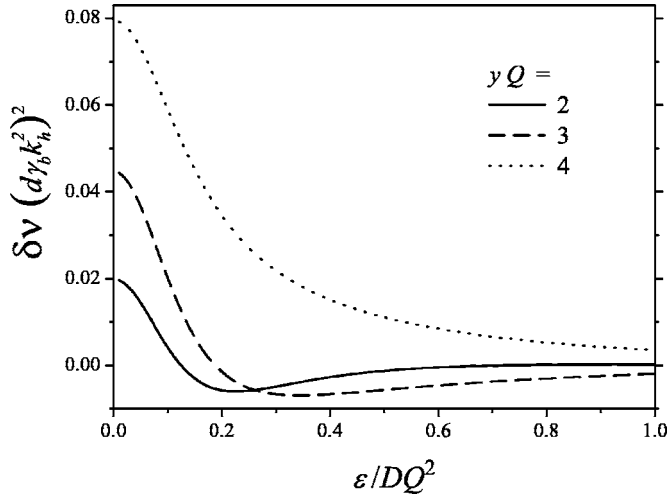
FIG. 6. Correction $\delta\nu(\varepsilon)$ to the DOS at the free surface of the F layer in the case of positive chirality. The curves are plotted at several points y. Other parameters are the same as in Fig. 5.

supplement the figures from Ref. 28 and demonstrate that $\delta\nu(0) > 0$.

Figure 5 is plotted for the same parameters as Fig. 2 in Ref. 28 and shows the spatial dependence of the DOS inside a domain (y is counted from the center of the domain) at several energies. Indeed, the DOS at low energies becomes positive everywhere.

Figure 6 illustrates the $\delta\nu(\varepsilon)$ dependence at several points y. In accordance with Ref. 41, the zero-energy correction to the DOS is positive forming the zero-energy peak.

V. DISCUSSION

In our study we neglected orbital effects of the magnetic field in the ferromagnet. Below we demonstrate that this is justified for thin F films. We also estimate the influence of the spin-orbit interaction on the LRTC. Finally, we comment upon the role of the boundary conditions at the SF interfaces in our problem.

The magnetization **M** in the F layer leads to the appearance of the vector potential **A** which can be estimated as $A \sim 4\pi M d$. The vector potential enters Eq. (8) as an additional term $(2\pi A/\phi_0)^2$, where $\phi_0 = hc/2e$ is the magnetic flux quantum. This term will restrict the penetration length of the LRTC if it is larger than the term $2k_\omega^2 = 2|\omega|/D \sim 2\pi T/D$. In the opposite limit

$$\left(\frac{8\pi^2 M d}{\phi_0}\right)^2 < \frac{2\pi T}{D} \tag{75}$$

one can neglect the orbital effects (the effect of Meissner currents on the LRTC). Taking $M \sim 50$ G, $T \sim 5$ K, and $D \sim 10$ cm²/s, we obtain $d < 300$ nm. Therefore the orbital effects can be neglected in the case of thin F layers. One can also show that under these conditions the Meissner currents induced in the superconductors by the stray magnetic fields are much smaller than the depairing currents. Therefore one can neglect the influence of the magnetic field of the ferro-

magnet on the amplitude of the order parameter in the superconductors. There is one more effect of the domain structure in the ferromagnet. This effect occurs in Josephson junctions with lateral dimensions larger than the Josephson length λ_J and is related to a spatial variation of the phase difference. Due to this a modulation of the total critical Josephson current arises. This effect was studied theoretically in Ref. 23.

If the spin-orbit interaction is present in the F layer, it leads to a decrease of the LRTC penetration length.[3] In this case the wave vector k_ω^2 should be replaced by $k_\omega^2 + 4/\tau_{SO}D$, where τ_{SO} is the spin-orbit relaxation time. Thus, the LRTC penetration length cannot be larger than $\sqrt{\tau_{SO}D/8}$.

Note also that we use boundary conditions (10) which follow from the Kupriyanov-Lukichev ones and describe spin-conserving interfaces with potential barriers. These boundary conditions themselves do not lead to the appearance of the LRTC in the uniform ferromagnet. In some papers spin-active interfaces were studied.[42,43] The scattering at such interfaces can generate the LRTC even in the uniform ferromagnet (see Ref. 44, and references therein). The boundary conditions for the spin-active interfaces were written in terms of a phenomenological scattering matrix. The microscopic calculation of the scattering matrix is lacking and the properties of spin-active SF interfaces in experiment are not known at present.

In a recent paper Ref. 45 the LRTC was analyzed numerically in a model of a SFS structure with a half-metallic ferromagnet and spin-active interfaces. The exchange field near the SF interfaces was assumed to be inclined with respect to the exchange field in the bulk of the ferromagnetic layer. To some extent this model is similar to a model of SF structure with a domain wall at the SF interface analyzed in Ref. 11. Therefore, the spin-active interfaces are additional sources of the LRTC in the ferromagnet. In order to single out the effect of the Néel domain walls on the LRTC, we did not consider the spin-active interfaces.

VI. CONCLUSIONS

We have studied a Josephson junction between two superconductors through a multidomain ferromagnet (F) with an in-plane magnetization, assuming that the neighboring domains are separated by the Néel domain walls. Due to an inhomogeneous magnetization, the long-range triplet superconducting component (LRTC) arises in the system. Arising at the domain walls, this component spreads into domains over a long distance of the order $\xi_T = \sqrt{D/2\pi T}$, which is much greater than the usual short length $\xi_h = \sqrt{D/h}$ describing the decaying of superconducting correlations in a ferromagnet with a homogeneous magnetization.

We have calculated the Josephson current due to this component in the case when the short-range components exponentially decay over the thickness of the F layer and can be neglected. Focusing on the limit when the F layer is thin from the viewpoint of the long-range component we find that the junction is in the π state. The LRTC does not oscillate inside the F layer, while the additional π phase of the condensate wave function is due to $\pi/2$ shifts at the SF interfaces. This interpretation suggests that the junction must be

in the π state due to the LRTC regardless of the F layer's thickness. When the F layer is not thin (from the viewpoint of the LRTC), analytical expressions for the supercurrent become cumbersome, however, numerical calculations indicate that the junction is indeed in the π state.

The absolute value of the Josephson current density is maximal at the boundaries between domains and domain walls, see Fig. 2. The current mainly flows along these lines.

We have considered two possible chiralities of the domain structure (positive and negative), which are determined by the relative orientation of rotating magnetizations in the neighboring domain walls. The absolute value of the Josephson current due to the LRTC is larger in the case of the negative chirality, because this case corresponds to a more inhomogeneous magnetization.

Analyzing a correction to the density of states due to the LRTC, we find that at zero energy (i.e., at the Fermi level) the correction is positive. This fact is in accordance with the general statement from Ref. 41, based on the odd frequency dependence of the Green function.

*Electronic address: fominov@landau.ac.ru

†Electronic address: volkov@tp3.rub.de

[1] A. I. Buzdin, Rev. Mod. Phys. **77**, 935 (2005).

[2] I. F. Lyuksyutov and V. L. Pokrovsky, Adv. Phys. **54**, 67 (2005).

[3] F. S. Bergeret, A. F. Volkov, and K. B. Efetov, Rev. Mod. Phys. **77**, 1321 (2005).

[4] P. G. de Gennes, *Superconductivity of Metals and Alloys* (Benjamin, New York, 1966).

[5] A. A. Golubov, M. Yu. Kupriyanov, and E. Il'ichev, Rev. Mod. Phys. **76**, 411 (2004).

[6] V. V. Ryazanov, V. A. Oboznov, A. Yu. Rusanov, A. V. Veretennikov, A. A. Golubov, and J. Aarts, Phys. Rev. Lett. **86**, 2427 (2001).

[7] T. Kontos, M. Aprili, J. Lesueur, F. Genêt, B. Stephanidis, and R. Boursier, Phys. Rev. Lett. **89**, 137007 (2002).

[8] Y. Blum, A. Tsukernik, M. Karpovski, and A. Palevski, Phys. Rev. Lett. **89**, 187004 (2002).

[9] A. Bauer, J. Bentner, M. Aprili, M. L. Della-Rocca, M. Reinwald, W. Wegscheider, and C. Strunk, Phys. Rev. Lett. **92**, 217001 (2004).

[10] H. Sellier, C. Baraduc, F. Lefloch, and R. Calemczuk, Phys. Rev. Lett. **92**, 257005 (2004).

[11] F. S. Bergeret, A. F. Volkov, and K. B. Efetov, Phys. Rev. Lett. **86**, 4096 (2001).

[12] A. Kadigrobov, R. I. Shekhter, and M. Jonson, Europhys. Lett. **54**, 394 (2001).

[13] V. L. Berezinskii, Pis'ma Zh. Eksp. Teor. Fiz. **20**, 628 (1974) [JETP Lett. **20**, 287 (1974)].

[14] V. T. Petrashov, V. N. Antonov, S. V. Maksimov, and R. Sh. Shaikhaidarov, Pis'ma Zh. Eksp. Teor. Fiz. **59**, 523 (1994) [JETP Lett. **59**, 551 (1994)].

[15] M. D. Lawrence and N. Giordano, J. Phys.: Condens. Matter **8**, L563 (1996).

[16] M. Giroud, H. Courtois, K. Hasselbach, D. Mailly, and B. Pannetier, Phys. Rev. B **58**, R11872 (1998).

[17] V. T. Petrashov, I. A. Sosnin, I. Cox, A. Parsons, and C. Troadec, Phys. Rev. Lett. **83**, 3281 (1999).

[18] V. Peña, Z. Sefrioui, D. Arias, C. Leon, J. Santamaria, M. Varela, S. J. Pennycook, and J. L. Martinez, Phys. Rev. B **69**, 224502 (2004).

[19] P. Nugent, I. Sosnin, and V. T. Petrashov, J. Phys.: Condens. Matter **16**, L509 (2004).

[20] D. Stamopoulos, N. Moutis, M. Pissas, and D. Niarchos, Phys. Rev. B **72**, 212514 (2005).

[21] R. S. Keizer, S. T. B. Goennenwein, T. M. Klapwijk, G. Miao, G. Xiao, and A. Gupta, Nature (London) **439**, 825 (2006).

[22] I. Sosnin, H. Cho, V. T. Petrashov, and A. F. Volkov, Phys. Rev. Lett. **96**, 157002 (2006).

[23] A. F. Volkov, A. Anishchanka, and K. B. Efetov, Phys. Rev. B **73**, 104412 (2006).

[24] A. F. Volkov, F. S. Bergeret, and K. B. Efetov, Phys. Rev. Lett. **90**, 117006 (2003).

[25] F. S. Bergeret, A. F. Volkov, and K. B. Efetov, Phys. Rev. B **68**, 064513 (2003).

[26] A. Aharoni, *Introduction to the Theory of Ferromagnetism* (Oxford, New York, 2001).

[27] T. Champel and M. Eschrig, Phys. Rev. B **71**, 220506(R) (2005); **72**, 054523 (2005).

[28] A. F. Volkov, Ya. V. Fominov, and K. B. Efetov, Phys. Rev. B **72**, 184504 (2005).

[29] M. Eschrig, J. Kopu, J. C. Cuevas, and G. Schön, Phys. Rev. Lett. **90**, 137003 (2003).

[30] F. S. Bergeret, A. F. Volkov, and K. B. Efetov, Phys. Rev. B **64**, 134506 (2001).

[31] Ya. M. Blanter and F. W. J. Hekking, Phys. Rev. B **69**, 024525 (2004).

[32] L. P. Gor'kov and V. Z. Kresin, Physica C **367**, 103 (2002).

[33] I. V. Bobkova, P. J. Hirschfeld, and Yu. S. Barash, Phys. Rev. Lett. **94**, 037005 (2005).

[34] G. A. Ovsyannikov, I. V. Borisenko, P. V. Komissinskii, Yu. V. Kislinskii, and A. V. Zaitsev, Pis'ma Zh. Eksp. Teor. Fiz. **84**, 320 (2006) [JETP Lett. **84**, 262 (2006)].

[35] F. S. Bergeret, K. B. Efetov, and A. I. Larkin, Phys. Rev. B **62**, 11872 (2000).

[36] D. A. Ivanov and Ya. V. Fominov, Phys. Rev. B **73**, 214524 (2006).

[37] M. Yu. Kuprianov and V. F. Lukichev, Zh. Eksp. Teor. Fiz. **94**, 139 (1988) [Sov. Phys. JETP **67**, 1163 (1988)].

[38] We employ the formula $\Sigma_{k=1}^{\infty} \sin((2k-1)x)/(2k-1) = \pi/4$ (at $0 < x < \pi$), see I. S. Gradshteyn and I. M. Ryzhik, *Table of Integrals, Series, and Products* (Academic, New York, 1965).

[39] Actually, the supercurrent in the limit $a_0 \to 0$ does not vanish exactly, but is determined by an exponentially small contribution from the short-range component which we neglect in this paper.

[40] A. A. Golubov, M. Yu. Kupriyanov, and Ya. V. Fominov, Pis'ma Zh. Eksp. Teor. Fiz. **75**, 223 (2002) [JETP Lett. **75**, 190 (2002)].

[41] Y. Tanaka and A. A. Golubov, Phys. Rev. Lett. **98**, 037003 (2007).

[42] A. Millis, D. Rainer, and J. A. Sauls, Phys. Rev. B **38**, 4504 (1988).

[43] E. Zhao, T. Löfwander, and J. A. Sauls, Phys. Rev. B **70**, 134510 (2004).

[44] M. Eschrig, T. Löfwander, T. Champel, J. C. Cuevas, J. Kopu, and G. Schön, cond-mat/0610212.

[45] Y. Asano, Y. Tanaka, and A. A. Golubov, Phys. Rev. Lett. **98**, 107002 (2007).